Registry No. Butyrate, 107-92-6.

REFERENCES

Bates, D. L., & Thomas, J. O. (1981) *Nucleic Acids Res. 9*, 5883–5894.

Benjamin, W. B. (1971) *Nature (London), New Biol. 234*, 18–20.

Candido, E. P., Reeves, R., & Davie, J. R. (1978) *Cell (Cambridge, Mass.) 14*, 105–113.

Cole, R. D. (1984) *Anal. Biochem. 136*, 24–30.

Covault, J., Sealy, L., Schnell, R., Shires, A., & Chalkley, R. (1982) *J. Biol. Chem. 257*, 5809–5815.

D'Anna, J. A., Gurley, L. R., Becker, R. R., Barham, S. S., Tobey, R. A., & Walters, R. A. (1980a) *Biochemistry 19*, 4331–4341.

D'Anna, J. A., Tobey, R. A., & Gurley, L. R. (1980b) *Biochemistry 19*, 2656–2671.

D'Anna, J. A., Gurley, L. R., & Tobey, R. A. (1982) *Biochemistry 21*, 3991–4001.

Gjerset, R., Gorka, C., Hasthorpe, S., Lawrence, J. J., & Eisen, H. (1982) *Proc. Natl. Acad. Sci. U.S.A. 79*, 2333–2337.

Gurley, L. R., & Hardin, J. M. (1969) *Arch. Biochem. 130*, 1–6.

Hall, J. M., Davis, C., & Cole, R. D. (1985) *FEBS Lett. 189*, 92–96.

Hohmann, P., & Cole, R. D. (1971) *J. Mol. Biol. 58*, 533–540.

Hurley, C. K. (1977) *Anal. Biochem. 80*, 624–626.

Keppel, F., Allet, B., & Eisen, H. (1977) *Proc. Natl. Acad. Sci. U.S.A. 74*, 653–656.

Laemmli, U. K. (1970) *Nature (London) 227*, 680–685.

Lennox, R. W. (1984) *J. Biol. Chem. 259*, 669–672.

Panyim, S., & Chalkley, R. (1969) *Biochem. Biophys. Res. Commun. 37*, 1042–1049.

Pehrson, J. P., & Cole, R. D. (1980) *Nature (London) 285*, 43–44.

Pehrson, J. R., & Cole, R. D. (1982) *Biochemistry 21*, 456–460.

Plumb, M., Marashi, F., Green, L., Zimmerman, A., Zimmerman, S., Stein, J., & Stein, G. (1984) *Proc. Natl. Acad. Sci. U.S.A. 81*, 434–438.

Robbins, E., & Borun, T. W. (1967) *Proc. Natl. Acad. Sci. U.S.A. 57*, 409–416.

Ruderman, J. V., Baglioni, C., & Gross, P. R. (1974) *Nature (London) 247*, 36–38.

Sealy, L., & Chalkley, R. (1978) *Cell (Cambridge, Mass.) 14*, 115–121.

Stellwagon, R. H., & Cole, R. D. (1969) *J. Biol. Chem. 244*, 4878–4887.

Varricchio, F., Mabojunje, O., Kim, D., Furtner, J. G., & Fitzgerald, P. J. (1977) *Cancer Res. 37*, 3964–3969.

Zweidler, A. (1980) *Dev. Biochem. 15*, 47–56.

A Nonuniform Distribution of Excision Repair Synthesis in Nucleosome Core DNA†

Suey Y. Lan and Michael J. Smerdon*

Biochemistry/Biophysics Program, Washington State University, Pullman, Washington 99164-4660

Received May 3, 1985

ABSTRACT: We have investigated the distribution in nucleosome core DNA of nucleotides incorporated by excision repair synthesis occurring immediately after UV irradiation in human cells. We show that the differences previously observed for whole nuclei between the DNase I digestion profiles of repaired DNA (following its refolding into a nucleosome structure) and bulk DNA are obtained for isolated nucleosome core particles. Analysis of the differences obtained indicates that they could reflect a significant difference in the level of repair-incorporated nucleotides at different sites within the core DNA region. To test this possibility directly, we have used exonuclease III digestion of very homogeneous sized core particle DNA to "map" the distribution of repair synthesis in these regions. Our results indicate that in a significant fraction of the nucleosomes the 5′ and 3′ ends of the core DNA are markedly enhanced in repair-incorporated nucleotides relative to the central region of the core particle. A best fit analysis indicates that a good approximation of the data is obtained for a distribution where the core DNA is uniformly labeled from the 5′ end to position 62 and from position 114 to the 3′ end, with the 52-base central region being devoid of repair-incorporated nucleotides. This distribution accounts for all of the quantitative differences observed previously between repaired DNA and bulk DNA following the rapid phase of nucleosome rearrangement when it is assumed that linker DNA and the core DNA ends are repaired with equal efficiency and the nucleosome structure of newly repaired DNA is identical with that of bulk chromatin. Furthermore, the 52-base central region that is devoid of repair synthesis contains the lowest frequency cutting sites for DNase I in vitro, as well as the only "internal" locations where two (rather than one) histones interact with a 10-base segment of each DNA strand.

The process of nucleotide excision repair of DNA involves a "cut-and-patch" mechanism where a small region (containing the lesion) is excised and the resulting gap is filled by repair synthesis [see reviews by Lieberman (1976), Hanawalt (1977), Hanawalt et al. (1979), and Setlow (1980)]. Since the DNA in eukaryotes is organized into chromatin [for recent reviews on chromatin structure, see Cartwright et al. (1982), Igo-Kemenes et al. (1982), and Reeves (1984)], an integral feature of the repair process must be the interaction of repair enzymes with this tightly folded structure. Indeed, several different laboratories have now shown that, following damage of

† This study was supported by NIH Grant ES02614. M.J.S. is the recipient of an NIH Research Career Development Award.

0006-2960/85/0424-7771$01.50/0 © 1985 American Chemical Society

mammalian cells in culture with either UV[1] radiation (Smerdon & Lieberman, 1978, 1980; Smerdon et al., 1979; Williams & Friedberg, 1979; Bodel & Cleaver, 1981; Smerdon, 1983), bulky chemicals (Tlsty & Lieberman, 1978; Oleson et al., 1979; Zolan et al., 1982), or small alkylating agents (Sidik & Smerdon, 1984), the newly repaired DNA undergoes a transition from a highly nuclease-sensitive state to a much more nuclease-resitant state. Immediately after repair synthesis, the newly repaired DNA is rapidly digested by both staphylococcal nuclease and DNAse I, is not associated with isolated nucleosome core DNA, and does not yield the ~10-base repeat pattern on gels following DNase I digestion of nuclei. With a half-life of ~20 min, these regions become increasingly nuclease resistant, are associated with nucleosome cores and histone H1, and yield the ~10-base repeat pattern following DNase I digestion (Smerdon & Lieberman, 1980; Smerdon et al., 1982a). These results can be explained by a process involving the "unfolding" of DNA during excision repair to produce an "open", nonnucleosomal structural followed by the "refolding" of this DNA back to the native, or near native, structure (Lieberman et al., 1979). Data on the distribution and removal of bulky chemical adducts (Oleson et al., 1979; Kaneko & Cerutti, 1980, 1982; Jack & Brookes, 1982) and UV-induced pyrimidine dimers (Williams & Friedberg, 1979; Niggli & Cerutti, 1982) support this unfolding–refolding model.

One, yet unexplained, feature of this "nucleosome rearrangement" process is that following the rapid refolding of repaired DNA into a nucleosome structure the overall nuclease sensitivity of this DNA is not reduced to that of bulk DNA (Smerdon & Lieberman, 1978, 1980; Tlsty & Lieberman, 1978; Smerdon et al., 1979; Oleson et al., 1979). For instance, the ratio of the fraction of repair-incorporated nucleotdies rapidly digested by staphylococal nuclease or DNAse I to the fraction of rapidly digested bulk DNA decreases from a value of 3–5 (depending on the digestion conditions) for the unfolded state to a value of 1.3–1.8 for the folded state. This ratio then continues to decrease at a much slower rate and is still above 1.2 after 24 h. A similar pattern is observed for the increase in repair-incorporated nucleotides associated with isolated core DNA (Smerdon & Lieberman, 1978; Tlsty & Lieberman, 1978; Oleson et al., 1979). After the rapid rearrangement phase, the ratio of repair-incorporated nucleotides to bulk DNA in nucleosome core particles is 0.8–0.95 (again, depending on digestion conditions). Both this ratio and the ratio for nuclease-sensitive DNA (above) should be 1.0 for a completely uniform distribution of repair synthesis in native nucleosome structures. Therefore, immediately after the rapid phase of nucleosome rearrangement, either the conformation of nucleosomes formed in newly repaired regions differs from that of bulk chromatin, or the distribution of repair synthesis in nucleosomal DNA is nonuniform, *and* this nonuniformity is "preserved" during the refolding process. Since we have shown that histone H1 is present in most or all of these nucleosomes immediately following the refolding process, the differences that exist cannot be explained by a simply a difference in histone H1 content in these regions (Smerdon et al., 1982a). Furthermore, although staphylococcal nuclease digests a larger fraction of newly repaired DNA (to acid-soluble form) than bulk DNA following the rapid refolding event, the nucleosome repeat length of the repair-labeled DNA is the same as that of the bulk DNA following different extents of digestion (Smerdon & Lieberman, 1980). This latter observation indicates that the linker DNA regions of nucleosomes in the nascent chromatin have the *same* sensitivity to staphylococcal nuclease as the linker regions of nucleosomes in bulk chromatin. Thus, if the nucleosome structure in newly repaired regions of chromatin differs from that in bulk chromatin, the difference most likely resides in the core region of these nucleosomes.

A further clue to the understanding of the difference(s) between nucleosomes in newly repaired regions and those in bulk chromatin came from the gel profiles of the DNA fragments generated by DNase I digests of whole nuclei. As mentioned above, following the rapid refolding event, the DNase I digestion products from repair-labeled DNA have the same ~10-base repeat as those from bulk chromatin (Smerdon & Lieberman, 1980). However, we noted in that paper that the relative areas of the individual peaks in the repair-labeled DNA profiles were different than those in the corresponding bulk DNA profiles. Since this was true for extensive digests of the nuclei by DNase I, the results again indicated that the difference(s) between the newly repaired DNA and bulk DNA nucleosomes were due to differences in the core DNA region.

In this paper, we have extended the DNase I digestion studies to isolated core particles and show that the differences in the digestion profiles of repaired and bulk DNA are preserved in these core particle preparations. To determine if these differences (and those discussed above) are due to a nonuniform distribution of repair patches in nucleosome DNA, we have developed a method, using exonuclease III, to "map" the distribution of repair synthesis in homogeneous populations of 146-bp core DNA. The results indicate that repair synthesis occurring immediately after UV damage has a marked preference for the outer ~60 bases at the 5′ end and the outer ~30 bases at the 3′ end of the core DNA. We show that such a distribution of repair-incorporated nucleotides in native nucleosome structures can account for all the above-mentioned differences (and similarities) between newly repaired regions of chromatin and bulk chromatin.

Materials and Methods

Cell Culture and Labeling during Replicative Synthesis. Human diploid fibroblasts (strains AG1518 and IMR 90) were grown in culture as described in Smerdon et al. (1982b). Cells, between passage 10 and passage 17, were split 1:3 and prelabeled for 1 week with 25–75 nCi/mL [^{14}C]dThd (50 mCi/mmol; New England Nuclear), depending on the experiment. The medium was then changed with fresh medium, and the cells were incubated for 1 more week, at which point they were confluent.

Irradiation and Labeling during Repair Synthesis. Prior to irradiation, the confluent cells were treated with either 0 or 2 mM hdyroxyurea for 45 min. The cells were then irradiated with 12 J/m^2 UV light (predominantly 254 nm) at an incident dose of 2 W/m^2, as previously described (Smerdon et al., 1978). Immediately after irradiation, 10 μCi/mL [^{3}H]dThd (50–80 Ci/mmol; New England Nuclear) was added to the medium, and the cells were incubated for 30 min. The cells were then harvested immediately or incubated for varying times in conditioned medium, containing 50 μM dThd, prior to harvest (chased). Control cells were treated identically except the irradiation step was omitted.

Preparation of Core Particles for DNase I Digestions. For the preparation of nucleosome core particles, nuclei were prepared as described in Lawson & Cole (1979) [also see Smerdon & Lieberman (1981)] and suspended in buffer A (50 mM Tris, pH 7.5, 25 mM KCl, 1 mM $MgCl_2$, 1 mM $CaCl_2$, and 0.25 M sucrose). Nuclei [(1–2) × 10^6/mL] were then incubated at 37 °C with 0.5–1 unit/mL staphylococcal

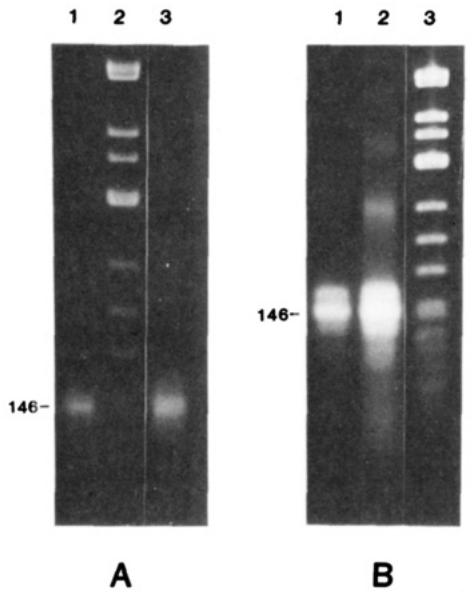

FIGURE 1: Agarose gels of core DNA from the two different core particle preparations. (A) Core particles used for the DNase I digestion studies. Nuclei were digested with staphylococcal nuclease in the higher ionic strength buffer (Materials and Methods) and the core particles isolated on sucrose gradients. Photograph shows DNA from isolated core particles (lane 1) and total digested DNA (lane 3). (B) Core particles used for the exonuclease III digestion studies. Nuclei were digested with staphylococcal nuclease in low ionic strength buffer (Materials and Methods) and the core particles isolated on sucrose gradients. Photograph shows DNA from isolated core particles (lane 1) and total digested DNA (lane 2). In each gel, the marker DNA fragments [lane 2 in (A) and lane 3 in (B)] were a *Hin*fI digest of ϕX 174 RF DNA. The numbers indicate the positon of the 146-bp fragments in each gel.

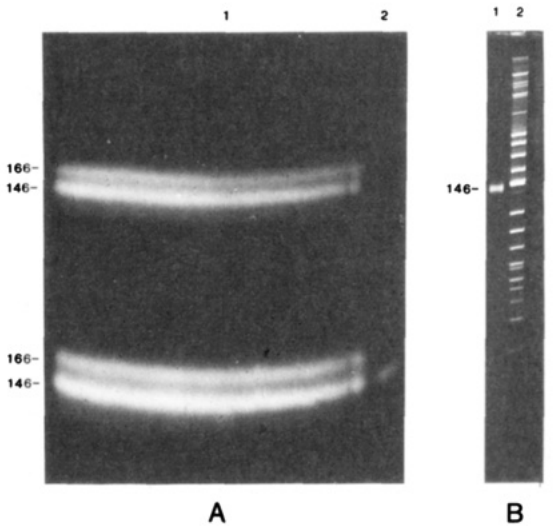

FIGURE 2: (A) Preparative agarose gel of core particle DNA obtained from mononucleosomes isolated as in Figure 1B. Approximately 32 μg of DNA was added to the preparative well (lane 1) and electrophoresed for 3 h. Another 32 μg of DNA was then added, and the samples were electrophoresed an additional 8.5 h. A sample of 146-bp core DNA, isolated by electroelution from a previous preparative gel, was applied to a second well (lane 2) at the time of the first loading. The numbers indicate the position of the 146-bp and 166-bp bands for each sample loading. (B) Denaturing polyacrylamide gel of 146-bp core DNA used for exonuclease III digestion studies. The 146-bp DNA was electroeluted from a preparative agarose gel (A), and 1 μg was denatured and applied to the gel (lane 1). Lane 2 shows the pattern for a *Hin*fI digest of ϕX 174 RF DNA ($\sim$10 μg) and can be used for comparison of the 146-base core DNA band with homogenous-sized fragments in the same concentration range. We note that some of the bands in this pattern represent restriction fragments that reannealed during the gel run (see Materials and Methods).

nuclease (14.9 units/μg; Worthington) until $\sim$25% of the bulk DNA label (^{14}C) was rendered acid-soluble. [Measurements of acid-soluble radioactivity were performed as described in Smerdon et al. (1978).] The reaction was stopped by addition of 10 mM EDTA (final concentration). Samples were then centrifuged at 300*g* for 2 min, and the supernatant was collected and dialysed vs. dialysis buffer [10 mM Tris, pH 7.8, 1 mM EDTA, and 0.1 mM phenylmethanesulfonyl fluoride (PMSF)]. From 1.5 to 2 mL of the supernatant was layered onto a 38-mL 5–20% sucrose gradient containing 2 mM EDTA and centrifuged at 49 000 rpm in a Beckman VTi50 vertical rotor for 3.5 h. The gradients were fractionated, and the fractions assayed for radioactivity. The monomer peak was then pooled and dialyzed vs. dialysis buffer. These core particle preparations were stored at 4 °C until used (usually less than 2 weeks). As shown in Figure 1A, the core particles from these preparations contained predominantly 146 bp of DNA. We note that we have tried a variety of published methods for obtaining core particles of more homogeneous DNA size, including selective precipitation [e.g., Simpson (1978)] and exonuclease trimming [e.g., Riley & Weintraub (1978)]. Unfortunately, none of these methods yielded a homogeneous core preparation from human fibroblast nuclei, and the above method consistantly gave the most homogeneous core particles. Furthermore, as discussed by Prunell & Kornberg (1982), the methods of selective precipitation of H1-containing core particles or trimming of core DNA with exonucleases could induce subtle rearrangements of the core particle structure. Such rearrangements could alter the distribution of repair synthesis in core DNA from that in the intact cell.

Preparation of Core DNA for Exonuclease III Digestions. To obtain large amounts of homogeneous-sized 146-bp core DNA (without inducing structural rearrangements in the DNA–histone complex), the following method was developed. Nuclei were isolated by the method outlined in Smerdon et al. (1979) and suspended in buffer B3 (10 mM Tris, pH 7.8, 0.1 mM $CaCl_2$, and 0.25 M sucrose). Staphylococcal nuclease digestion of human fibroblast nuclei in this low ionic strength, isotonic buffer yields discrete 146- and 166-bp core DNA bands without the "smearing" (or intermediate DNA sizes) that is observed when a higher ionic strength digestion buffer is used (Figure 1B). The nuclei were incubated with staphylococcal nuclease until 20–25% of the bulk DNA label (^{14}C) was rendered acid soluble, and the nucleosome monomers were purified on 5–20% sucrose gradients as described above. As shown in Figure 1B, the resulting monomers consist of a mixture of 146- and 166-bp core particles, as well as some cores with DNA degraded to "submonomer" sizes. After dialysis of the pooled monomer fractions (as above), the sample solution was concentrated to a volume of 1–3 mL (depending on the experiment) with an immersible ultrafiltration unit (Millipore, CX-10). [We note that several concentration methods were tested and this method gave the highest recoveries of core particles (i.e., 75–90%).] At this point, the DNA concentration was 35–40 μg/mL. The core DNA was prepared by incubation with 100 μg/mL proteinase K (EM Biochemicals) at 37 °C for $\sim$12 h, followed by ethanol precipitation (Smerdon et al., 1978; Smerdon & Lieberman, 1980). The core DNA was then electrophoresed on preparative 2.8% agarose slab gels (see below). We routinely used 30–40 μg of core DNA per loading and usually added a second sample to the same gel 2–3 h after the first sample was loaded (Figure 2A). The DNA was visualized with ethidium bromide (Smerdon et al., 1978), and the 146-bp bands were excised from the gel. The agarose slices were then cut into 5-cm

lengths (having a thickness and width of 4–5 mm) and placed in 7-mm (inner diameter) tubes filled to within ~7 cm from one end with 1.5% agarose in electrophoresis buffer (see below). The slices were then covered with additional 1.5% agarose, leaving a space of ~2 cm at the end of each tube. The space was filled with ~1 mL of electrophoresis buffer, and the end was sealed with dialysis membrane (Spectrapore No. 1, Spectrum Medical Industries, Inc.). The gels were subjected to 90 V for ~5 h, and the electrodes were then reversed for 5 min (to release DNA from the dialysis membrane). The buffer at the end of each tube, which now contained the core DNA, was removed with a syringe by first puncturing the membrane with the syringe needle. The remaining ethidium bromide bound to the DNA was extracted with water-saturated isobutyl alcohol (Prunell & Kornberg, 1977). The resulting DNA fragments were homogeneous in size on both native and denaturing gels (e.g., Figure 2) and did not contain any internal strand breaks.

Nuclease Digestions. Whole nuclei were digested with DNase I (Sigma; 2045 Kunitz units/mg) as described in Smerdon & Lieberman (1980). The DNase I digestions of isolated core particles (~40 μg of DNA/mL) were carried out at 37° C in either the dialysis buffer plus 2.1 mM $CaCl_2$ or buffer B3. Digestion times were from 4 to 20 min. After termination of the digestion with 10 mM EDTA, the DNA fragments were purified by proteinase K digestion and ethanol precipitation as described earlier.

Purified 146-bp core DNA was ethanol-precipitated and redissolved in 100–300 μL of 60 mM Tris, pH 8, 1 mM $MgCl_2$, and 1 mM 2-mercaptoethanol at a concentration of 100–150 μg/mL. The DNA samples were incubated at 37 °C with *Escherichia coli* exonuclease III (Bethesda Research Laboratories), at a final concentration of 1–3 units/μg of DNA, for 12–100 min. We note that these digestion conditions (i.e., low salt, 37 °C, and low enzyme to DNA ratios) were chosen to facilitate a less synchronous and less processive degradation of core DNA (Donelson & Wu, 1972; Wu et al., 1976; Thomas & Olivera, 1978) to yield digestion profiles with relatively large "spreads" in the DNA fragment distribution about the ~70-base maximum (e.g., Figure 7). This latter feature allowed for measurements of $^3H/^{14}C$ ratios to be made at DNA fragment lengths of 100–125 bases from the 3′ end, depending on the amount of radioactive label in the isolated core DNA (see Results). The digestions were terminated by addition of 10 mM EDTA, and the samples were incubated with proteinase K (as above). In some experiments, the samples were denatured and loaded directly onto denaturing gels (see below). The profiles from these samples indicated that the enzyme liberated mononucleotides during the digestion and, therefore, served as a test for the proper action of the exonuclease. (The enzyme was also tested for endonuclease activity by incubation with supercoiled φX 174 RF DNA for 60 min at 37 °C. We observed no conversion of the supercoiled DNA to either relaxed circles or linear DNA forms during this time period.) In other experiments the proteinase K digested samples were ethanol-precipitated, and the DNA was dissolved in sample buffer containing 98% formamide (Smerdon & Lieberman, 1980) prior to denaturation and loading on the gels. (Under these conditions, the mononucleotide band is absent.) The resulting gel profiles from the two different samples gave identical $^3H/^{14}C$ ratios across the gel.

Electrophoresis. Except during electroelution (described above), all agarose electrophoresis was performed on horizontal, 0.5 × 12.5 × 30 cm slab gels according to Smerdon et al. (1978) with the exception that the electrophoresis buffer was 50 mM Tris, pH 8.3, 50 mM acetate, and 10 mM EDTA [as suggested by Smith et al. (1983)]. The well size for preparative electrophoresis of core DNA was 1.5 × 100 mm. All gels were run at 100 V.

Denaturing gel electrophoresis was performed on 8% polyacrylamide–7 M urea 0.15 × 15 × 25 cm slab gels as described by Maniatis et al. (1975) with some modification (Smerdon & Lieberman, 1980). Samples were heated to 100 °C for 5 min and immediately loaded onto prewarmed gels (Garoff & Ansorge, 1981). Electrophoresis was carried out at 25 W for ~2.5 h. Several different DNA size markers were tested on these gels [including *Hinf*1 restriction fragments of φX174 RF DNA, *Hae*III restriction fragments of pBR 322 DNA, and a preparation of ligated linker DNA fragments (8 bases long)], and each was found to partially renature at the concentrations required for visualization by ethidium bromide (e.g., Figure 2B). Therefore, the gels were calibrated with fragments from a DNase I digest of 146-bp core particles, assuming the maximum of each peak to be an integer multiple of 10.4 bases (Prunell et al., 1979), and the bromophenol blue marker dye, which comigrates with 21-base fragments of DNA on these gels (Lutter, 1979; Smerdon & Lieberman, 1980). After electrophoresis, the gels were stained with ethidium bromide and photographed, and the gel lanes were sliced and solubilized as described in Smerdon & Lieberman (1980). The samples were assayed for radioactivity on a Beckman LS 7500 liquid scintillation counter equipped with a microprocessor. The ^3H and ^{14}C dpm were determined from the double-label computer program developed for this scintillation counting system (Beckman) following sample counting times of either 5 or 10 min per vial, depending on the level of radioactivity present. [The maximum error at 80 dpm above background (i.e., the minimum number of ^3H dpm used in these experiments) was ±18% (95% confidence limits).] Scans of the photographic negatives of ethidium bromide stained gels were obtained from a Helena Laboratories Quick-Scan R and D gel scanner equipped with a Quick Quant II integrator.

Integration of DNase I Digestion Profiles. Integration of the gel profile peaks was performed on a Nicolet computer using a program designed by Nicolet Technology Corp. (Fremont, CA) to integrate individual peaks in a multipeak NMR spectrum where the peaks are overlapping. This method fits each set of data with a series of peaks, which can be 100% Gaussian, 100% Lorentzian, or any linear combination of Gaussian and Lorentzian shapes. Furthermore, the "background function" (i.e., the functional dependence of background label with migration distance) can be constant or sloping. Thus the gel profiles were analyzed on a Nicolet 1280 computer using the NMCCAP program for curve analysis and deconvolution. The best fit (or lowest RMS value) was obtained from a basis spectrum line shape of 75% Gaussion and 25% Lorentzian. The relative area for each peak was then determined from the computed areas of the individual peaks in the basis spectrum. [See supplementary material for further details (see paragraph at end of paper regarding supplementary material).]

Curve Analysis of the Exonuclease III Digestion Data. Normalized ratio data obtained from the exonuclease III digestion of core DNA was fit with eq A3 and A4 of the Appendix by using an Apple IIe computer and a computer program written by C. Trindle for Project Seraphim. This program determines the best fit parameters by a nonlinear least-squares method (Bevington, 1969).

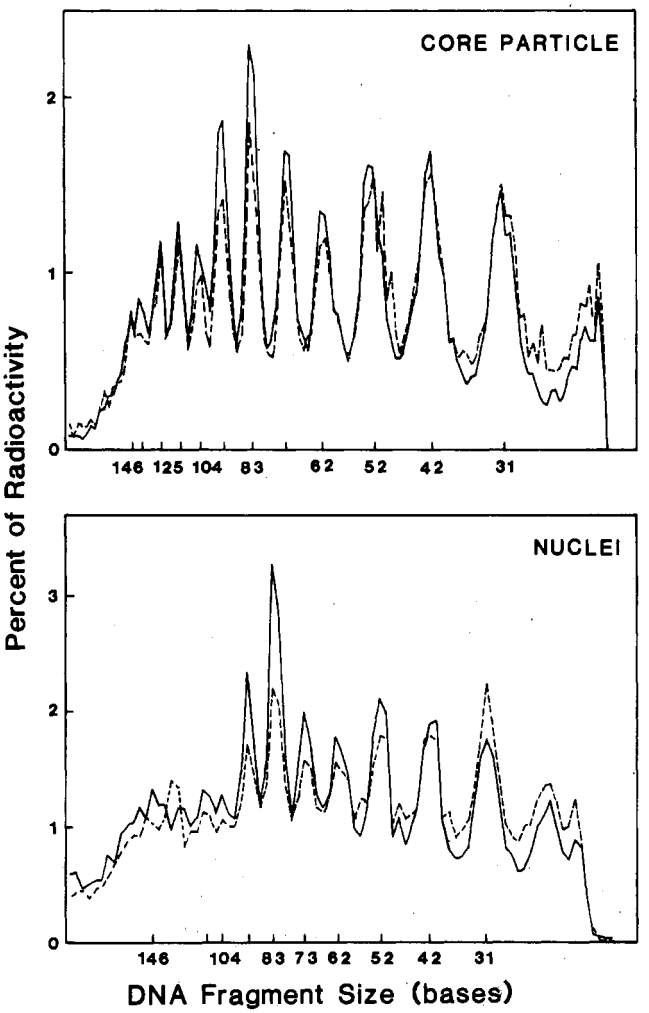

FIGURE 3: Denaturing gel profiles of DNase I digestion products from either isoalted core particles (upper panel) or nuclei (lower panel). Core particles were isolated from cells harvested immediately after the 30-min pulse-labeling period. Nuclei were isolated from cells pulse labeled for 30 min and chased for 4.75 h prior to harvest. Cells were labeled in the presence of 2 and 10 mM hydroxyurea for the core particle and nuclei preparations, respectively. In each panel, the solid line represents the ^{14}C profile (bulk DNA), and the dashed line represents the ^{3}H profile (newly repaired DNA), which has been corrected for the contribution of replicative synthesis (see supplementary material).

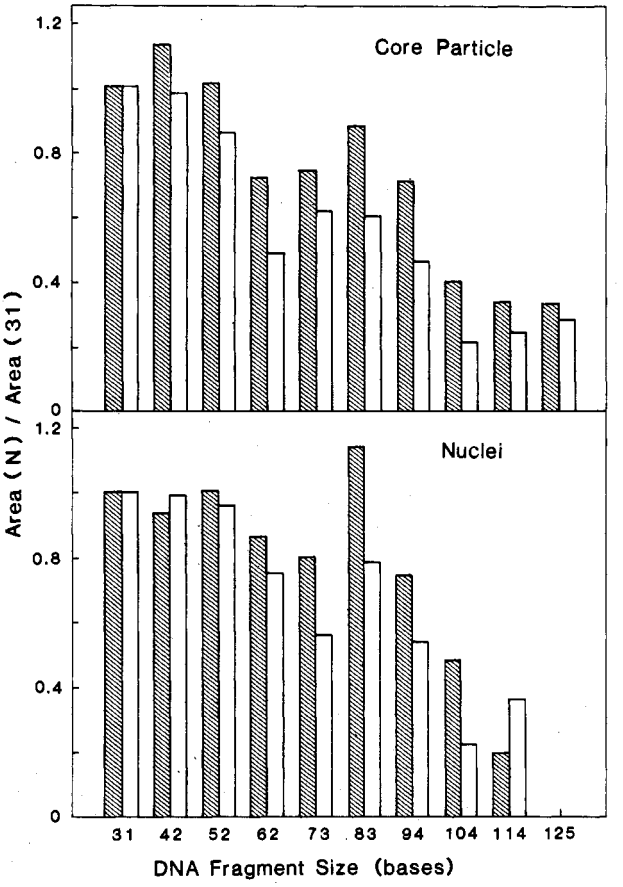

FIGURE 4: Relative mass fractions of the peaks in the DNase I digestion profiles shown in Figure 3. The areas of each peak (N) were determined as described under Materials and Methods and divided by the area for the 31-base peak. The values for the ^{14}C and ^{3}H peaks are denoted by the hatched and open bars, respectively. We note that the ^{14}C profiles of the two sets of data differ due to different extents of digestion in each case.

RESULTS

Analysis of DNase I Digestion Profiles. Core particles were prepared from human diploid fibroblasts that were prelabeled with [^{14}C]dThd, grown to confluence, irradiated with 12 J/m^2 UV light, and labeled for 30 min during the early, rapid phase of repair synthesis (Smerdon et al., 1978). Following digestion of the nuclei with staphylococcal nuclease, the core particles were isolated on sucrose gradients (Materials and Methods). As shown in Figure 3 (top panel), the digestion of these core particles with DNase I resulted in the expected ~10-base repeat pattern with a reduced background compared to that obtained for whole nuclei (Figure 3, bottom panel). Furthermore, careful inspection of the data in Figure 3 indicates that the areas (or mass fractions) for some of the peaks differ between the ^{3}H and ^{14}C profiles. For example, the areas for the 83- and 94-base peaks are less for the ^{3}H-labeled DNA than for the ^{14}C-labeled DNA, whereas the areas for the 42-base peak are similar for the two labels. The actual quantitative differences in the peak areas (relative to the area of the 31-base peak) for these profiles are shown in Figure 4, which gives the results of the peak area analysis. We note that the differences seen in Figure 4 are for one extent of digestion in each case. As discussed in the supplementary material, the difference pattern seen varied with the digestion extent. Furthermore, we note that although these differences are indeed small, they have been reproduced many times and for two different human fibroblast cell strains.

We then wished to determine what distribution(s) would be required for the small differences we observed, assuming that the nucleosomes in newly repaired regions have a native conformation, and would such a distribution be detectable by other methods. Therefore, we developed a method of analysis (described in the supplementary material) to determine the distribution of repair synthesis that would be required to yield the observed differences in the DNase I digestion profiles assuming the distribution fit one of the two models shown in Figure 5. The first model (model I) represents the case where repair synthesis occurs at any position within a region of the core DNA (bound by positions R1 and R2) with equal probability. The second model (model II) represents the case where repair synthesis occurs at the ends of the core DNA with equal probability and extends from the 5′ end to position R1 and from position R2 to the 3′ end. These models were chosen as the two most likely distributions of repair synthesis in a population of core particles, on the basis of considerations of the average size of "repair patches" (Francis et al., 1981; Th'ng & Walker, 1983) and the average separation of these patches in UV-damaged DNA (Williams & Cleaver, 1978; Niggli & Cerutti, 1982). It should be pointed out that these models do not require all repair patches to be the length of the "high-

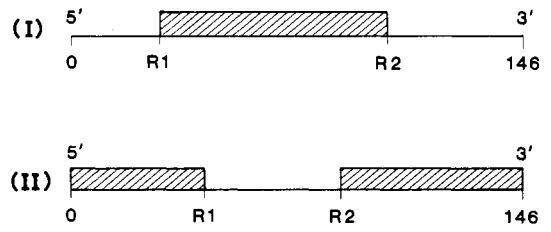

FIGURE 5: General models for the distribution of UV-induced excision repair synthesis in nucleosome core DNA. In each case, the region(s) containing repair-incorporated nucleotides is (are) denoted by the hatched bar(s) and is (are) bounded by positions R1 and R2. The R1 and R2 values given in the text are in bases from the 5′ end of the core DNA.

frequency" region (e.g., R2-R1 for model I). They simply require that, whatever the repair patch size, the patches occur with equal frequency at all sites within the designated region and not at all outside of this region. Clearly, these models may be oversimplifications of the actual distribution (e.g., repair synthesis may occur with a different probability at each site within core DNA); however, they serve to allow the determination of those regions of the core DNA that are relatively enhanced, and relatively devoid, of repair synthesis.

In summary, our procedure for performing the DNase I analyses involved correction of the ^3H data for the incorporation of label by replicative synthesis during the ^3H labeling period (see supplementary material) and determination of the relative areas of both the (corrected) ^3H and ^{14}C profiles (as above). The relative areas were then analyzed by a computer program that determined the correct set of fractions of different-sized DNA fragments generated by DNase I for a particular digestion time using the first-order rate constants determined by Lutter (1978) and the best fit of the relative peak areas for the ^{14}C profile. Assuming that the same set of fractions applies to the ^3H-labeled DNA (i.e., that cutting frequencies of DNase I within the core particles of newly repaired DNA are the same as those of bulk DNA), the analysis determines the values of R1 and R2 (Figure 5) that yield the best fits to the relative peak areas of the ^3H profile. The best fits for model I (Figure 5) were for R1 values in the range of 0–10 bases and R2 values in the range of 80–90 bases. The best fits for model II were for R1 values in the range of 40–50 bases and for R2 values in the range of 80–100 bases (supplementary material). Therefore, the best fits of the ^3H data from this analysis were obtained for distributions where some 40–60 bases of each strand of core DNA are devoid of repair synthesis. From these results, we conclude that the small differences observed in the DNase I digestion profiles could reflect significant differences in the levels of repair synthesis throughout the core region of the nucleosome. Furthermore, such differences in the distribution of repair synthesis should be readily detected by a direct measurement of the location of repair-incorporated nucleotides within core DNA.

Exonuclease III Mapping of the Distribution of Repair Synthesis in Nucleosome Core DNA. The method we have developed to determine the distribution of repair synthesis in nucleosome core DNA is schematically outlined in Figure 6. Once again, cells were prelabeled with [^{14}C]dThd during replicatie synthesis, grown to confluence, irradiated with 12 J/m^2 UV light, and labeled for 30 min during repair synthesis. To suppress replicative synthesis to very low levels during the ^3H-labeling period, the cells were treated with 2 mM hydroxyurea in most of the experiments (although cells not treated with this drug were also examined; see below). Initially, we examined core DNA from cells harvested immediately after the pulse-labeling period. In this case only those

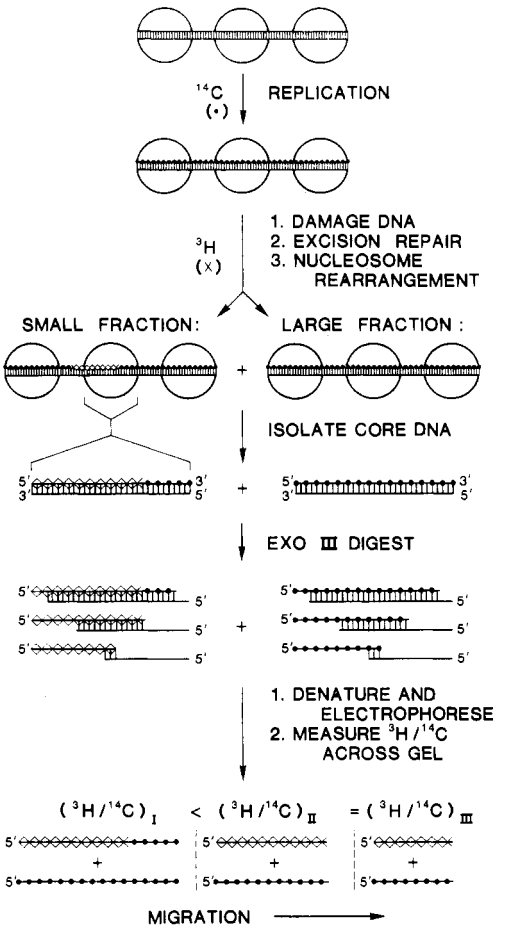

FIGURE 6: General scheme of the exonuclease III digestion experiments. Cells were labeled with [^{14}C]dThd during the growth phase, grown to confluence, irradiated with UV light, and labeled for 30 min (during repair) with [^3H]dThd, which is incorporated into a small fraction of the total DNA. Nuclei were isolated and digested with staphylococcal nuclease in low ionic strength, isotonic buffer producing mononucleosomes that are comprised of a large number of core particles uniformly labeled with ^{14}C and a small number of core particles containing ^3H (or newly repaired DNA). The mononucleosomes were isolated on sucrose gradients, and the 146-bp core DNA was isolated by preparative electrophoresis. The core DNA was then digested to different extents with exonuclease III, denatured, and electrophoresed on denaturing gels. The gel lanes were cut out, sliced, and assayed for radioactivity. The resulting ^3H dpm/^{14}C dpm profile across the gel was used as a measure of the distribution of excision repair synthesis in nucleosome core DNA. The example shown is for a nonuniform distribution where repair label is preferentially incorporated into the 5′ end of the core DNA.

regions that had undergone both repair *and* rearrangement back to a nucleosome structure during the labeling period would be isolated. Under the conditions used, this represents ~40% of the total label incorporated by repair synthesis. We then examined core DNA from cells pulse labled and chased for relatively short times. In this latter case, the core DNA included those regions that were repaired during the 30-min labeling time and refolded into a nucleosome structure *after* the labeling period (at this point 65–70% of the total repair incorporated label is associated with core DNA).

For these studies, homogeneous-sized, 146-bp core DNA was incubated with exonuclease III to yield DNA fragments containing the original 5′ termini and different-sized gaps at the 3′ ends (Figure 6). The fragments were then denatured and electrophoresed on denaturing gels. The amount of ^{14}C at a given fragment length is a measure of the total DNA of that size, and the amount of ^3H is a measure of the amount of repair-incorporated nucleotides within the DNA fragments

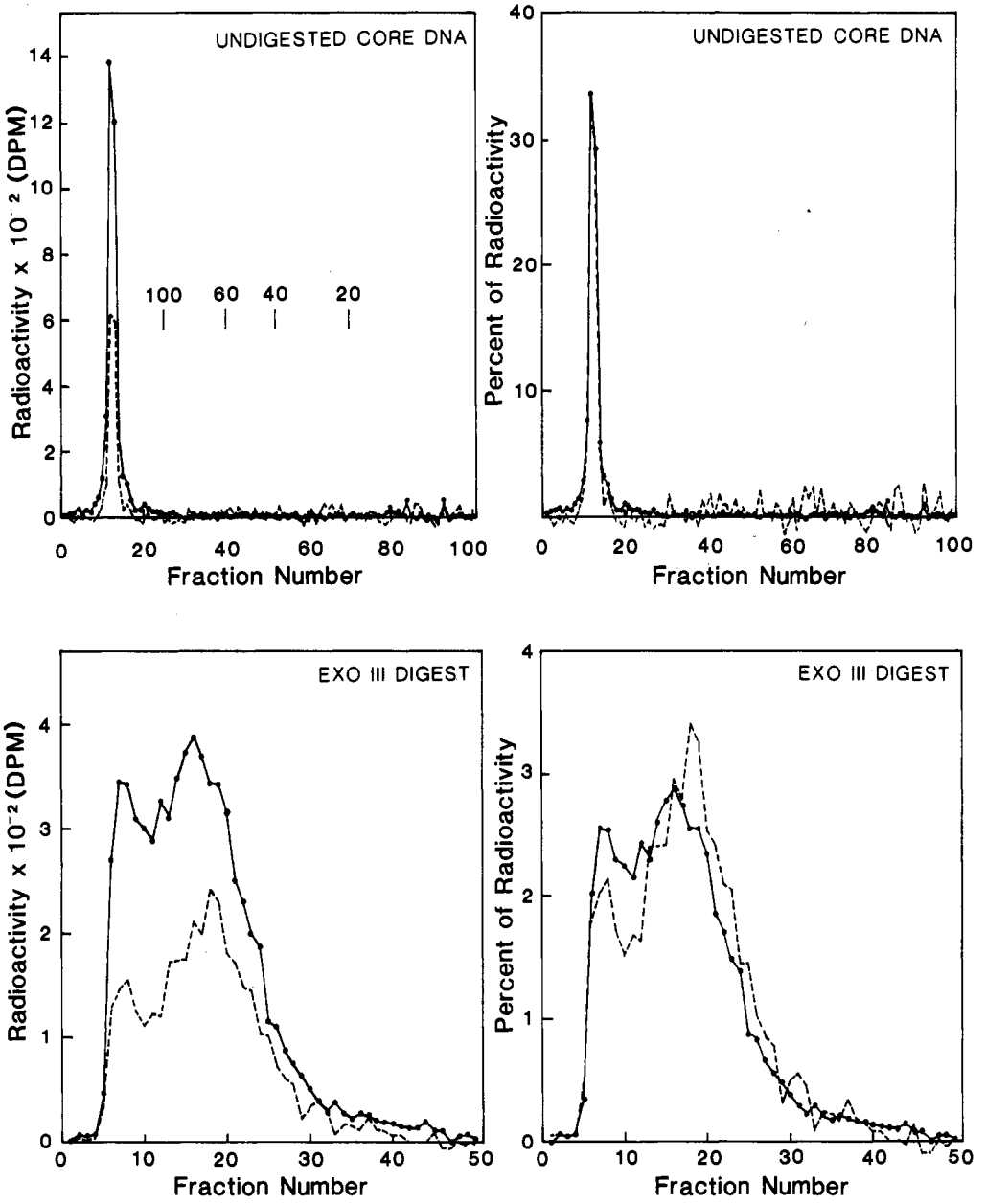

FIGURE 7: Radioactivity profiles for 146-bp core DNA either not digested (upper panels) or digested (lower panels) with exonuclease III and electrophoresed on a denaturing gel. The left-hand panels show the ^{3}H (dashed line) and ^{14}C (solid line) dpm, and the right-hand panels show the percent of total radioactivity loaded on the gel for each isotope. The numbers in the upper left panel indicate the positions of 20-, 40-, 60-, and 100-base fragments and can be used as markers for each of the panels since the abscissa values have been normalized to show the same length of gel as that in the upper left panel.

of that size. Therefore, the ratio of ^{3}H and ^{14}C across the gel profile can be used to determine the distribution of repair synthesis in the core DNA (see below). An example of a digestion profile for these experiments is shown in Figure 7. The data in the upper two panels is for undigested core DNA and shows that all of the ^{3}H-labeled DNA bands with the ^{14}C-labeled DNA. This result is consistent with recent findings from our laboratory that repair patches are ligated prior to folding into nucleosome core structures (Smerdon, 1985). Furthermore, as can be seen in the two lower panels, digestion with exonuclease III, as outlined under Materials and Methods, results in a broad distribution of DNA fragment sizes with a maximum in the distribution at ~70 bases. However, sufficient levels of radioactivity (i.e., >80 dpm above background) were obtained down to fragment sizes of ~40 bases (for cells harvested immediately after the pulse period) to ~20 bases (for cells chased following the pulse period). Thus, depending on the experiment, the level of repair synthesis could be determined for all but the 20–40 bases on the 5′ end of the core DNA.

It is helpful to plot the scintillation counting data as the percent of total radioactivity on the gel (Figure 7, right-hand panels). This normalization procedure allows direct graphical comparison of the ^{3}H and ^{14}C profiles. As seen in the example shown in Figure 7, the ^{3}H profile in the exonuclease III digested sample is shifted to smaller DNA fragment sizes and indicates that the distribution of repair synthesis is indeed nonuniform in the core DNA. The ratio of ^{3}H and ^{14}C vs. fraction number was measured for profiles such as these and compared for different extents of digestion with exonuclease III. We consistently obtained slightly lower values for these ratio curves for the early digestion times relative to those obtained for the late times where digestion was essentially complete (data not shown). The maximum shift observed was

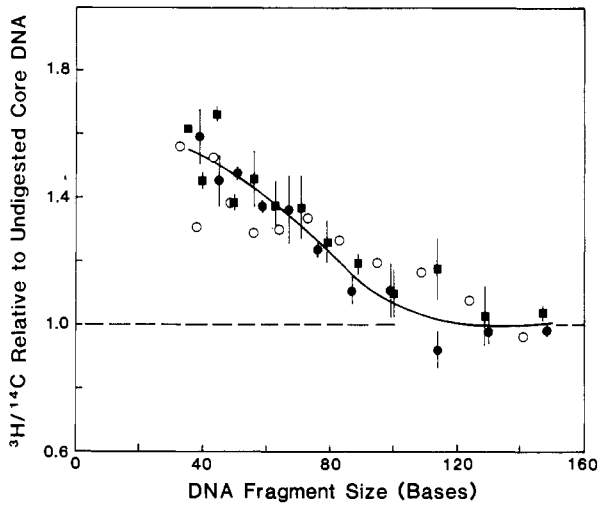

FIGURE 8: Ratio of ^3H and ^{14}C dpm as a function of DNA fragment size for exonuclease III digested 146-bp core DNA from cells harvested immediately after the pulse-labeling period. Different symbols represent three different core DNA preparations. Cells were labeled during repair synthesis in the presence (●, ■) or absence (○) of 2 mM hydroxyurea. Each value represents the average for either 2 (○) or 3 (●, ■) different digestion times obtained from profiles such as those in Figure 7. The error bars denote ± 1 SD of the mean. The values were normalized to the $^3H/^{14}C$ value for undigested core DNA in each case to allow direct comparison of the data from the three different core DNA preparations. The fit shown is to the solid symbols only. The dashed line denotes a random distribution of ^3H label.

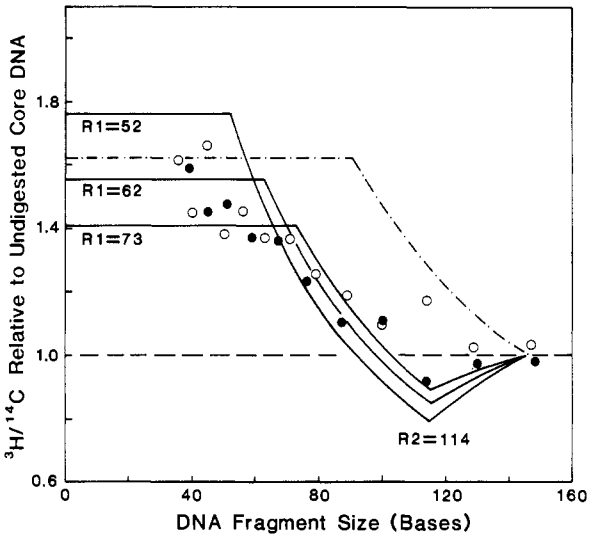

FIGURE 9: Theoretical fits of the data in Figure 8 based on the distribution models in Figure 5. The theoretical curves were generated as outlined in the Appendix. The solid lines show the best fits of the data for model II (i.e., for eq A3) and the corresponding values of R1 and R2. For comparison, we have included a theoretical curve for model I (i.e., eq A4), which corresponds to an R1 value of 0 and an R2 value of 90 (–·–). The open and closed circles correspond to the solid symbols in Figure 8.

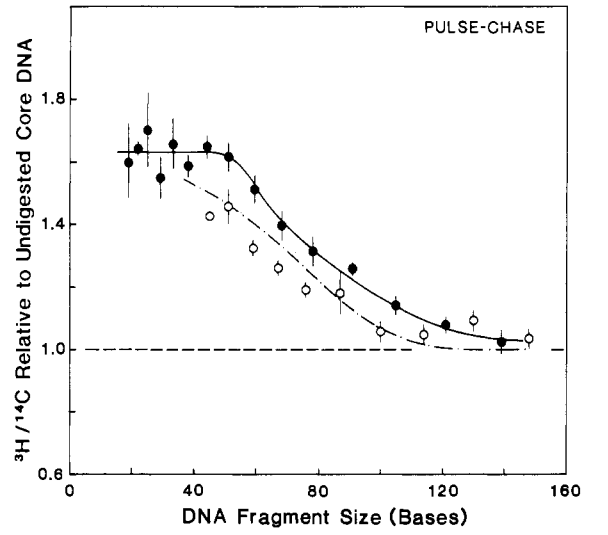

FIGURE 10: Normalized ratio curves for 146-bp core DNA from cells chased for short times after the pulse-labeling period. Cells were pulse-labeled in the presence (●) or absence (○) of 2 mM hydroxyurea and chased for 2.5 (●) or 4 h (○) prior to harvest. Data represent the mean ± 1 SD for three different exonuclease III digestion times. The solid line is a fit to the solid symbols, and the dashed-dotted line shows the fit to the solid symbols in Figure 8.

~10% and was insignificant relative to the overall change in the ratio values (see below). Therefore, we have simply averaged the values (at a given fragment size) for all the digestion times used and the values of $^3H/^{14}C$ represent the mean of this average in each case.

The results for cells pulse labeled in the presence or absence of 2 mM hydroxyurea and harvested immediately after the pulse period are shown in Figure 8. These data have been corrected for the contribution of DNA replicative synthesis to the total ^3H incorporated during the pulse period (see supplementary material). [Such a correction was essential for the analysis of core DNA from cells not treated with hydroxyurea [e.g., see Smerdon (1983)]; however, this correction could have been omitted for the hydroxyurea-treated cells since it yielded only a slight change in the ratio curves.] From these data, it is clear that the distribution of repair synthesis in core DNA is "weighted" toward the 5′ end, regardless of whether the cells were treated with hydroxyurea. Furthermore, the data remain at a value of close to 1.0 for fragment sizes in the range of ~120 bases to 146 bases and approximates a sigmoidal shape in going from 146 bases to smaller fragment sizes. This result suggests that repair-incorporated ^3H label is also located in the 3′ end of the core DNA. Thus, to a first approximation, the data in Figure 8 suggest a general distribution similar to model II in Figure 5. Given this model, one can calculate the expected $^3H/^{14}C$ curves for all values for R1 and R2 (see Appendix). Some examples of the curves obtained for different values of R1 and a single value of R2 (114 bases) are shown in Figure 9 (solid lines), along with a curve representing the case where no ^3H label is located on the 3′ end (dashed dotted line). (The latter curve demonstrates how rapid the data should increase from a value of 1.0 as the fragment size decreases from 146 bases when no ^3H label is located on the 3′ end.) From the theoretical curves shown in Figure 9, it can be seen that the distribution in model II yields normalized ratios that decrease from 1.0 in going to smaller DNA fragment sizes from 146 bases until the value of R2 is reached. At this point, the curves bend sharply upward to the value at R1 and then plateau for all smaller fragment sizes. Although these curves predict a similar shape to that of the ratio data, some quantitative differences should be noted. First of all, the data in the 100–146-base region do not decrease to the values predicted by the curves yielding the best fit to the data in the lower DNA size range. (This deviation may be due in part to the large gradient in DNA size vs. migration distance in this region of the gel.) Second, it is difficult to determine from the data in Figure 8 if the ratio levels off in the small DNA size range as predicted by model II.

Normalized ratios for core DNA from cells pulse labeled in the presence of hydroxyurea and chased for 2.5 h are shown in Figure 10 (closed circles). As discussed above, the core

DNA from these cells is labeled to a higher ^3H specific activity and allows determination of ratios down to ~20-base fragments. As can be seen, the dependence of the ratio on DNA fragment size is not very different from the fit to the data in the Figure 8 (i.e., for cells not chased prior to harvest) and plateaus at a value of ~1.6 in the low molecular region of the gel. This value is close to the value of 1.54 predicted by the fit shown in Figure 9 for an R1 value of 62 bases and an R2 value of 114 bases. Indeed, the data for five different experiments were analyzed by computer, using a nonlinear least-squares curve-fitting algorithm, the best fit values obtained for R1 and R2 (varied by 10.4-base increments) were 62 and 114 bases, respectively.

Figure 10 also includes data from cells not treated with hydroxyurea during the pulse-labeling period and chased for 4 h (open circle). As can be seen, the normalized ratio values for this core DNA are also similar to those obtained for cells that were not chased. Therefore, the presence of hydroxyurea does not appear to alter the overall distribution of repair synthesis in core DNA. Furthermore, the nonuniform distribution appears to "persist" in the cell for at least several hours after the incorporation of label by repair synthesis.

Discussion

These studies stem from a previous observation that, following the rapid refolding of newly repaired DNA into a nucleosome structure, the gel profiles of the repaired DNA were different from those of bulk DNA following extensive digestion of nuclei by DNase I (Smerdon & Lieberman, 1980). Although the DNA from newly repaired regions was cut with the same 10.4-base periodicity as bulk DNA, the mass fractions of each label (i.e., the areas under the peaks) were somewhat different. In this paper, we have shown that similar differences are obtained from isolated core particles (Figures 3 and 4 and supplementary material). Thus, the differences observed for the digestion of whole nuclei are, at least in part, preserved in the nucleosome core region of newly repaired DNA. As discussed in the introduction, these differences could arise from (1) sublte differences in the nucleosome structure of newly repaired regions of chromatin (following the rapid refolding event) or (2) a nonuniform distribution of repair-incorporated nucleotides in nucleosome core DNA. Analysis of the small differences observed in the DNase I digestion profiles indicated that they could result from significant differences in the levels of repair synthesis at different sites within the core DNA. Indeed, for the two different general distributions considered (Figure 5), the best fits to the data were obtained for a distribution where 40–60 bases of each core DNA strand are devoid of repair synthesis.

We have used exonuclease III digestion of homogeneous-sized core DNA samples to map the distribution or repair synthesis in these regions (Figure 6). We estimate that this core DNA represented no more than 70% of the total core DNA in the cell. Our samples most likely did not include those nucleosomes that are either very resistant to digestion to the 146-bp core particle by staphylococcal nuclease or degraded raplidy to submonomer fragments. Therefore, it should be kept in mind that the results from our exonuclease III analysis may not be representative of *all* nucleosomes associated with newly repaired DNA.

Another concern with this approach is the possibility that exonuclease III may selectively degrade those core DNAs containing the repair-incorporated label. Such a selection might result from the preferential repair of specific sequences in DNA [e.g., in long pyrimidine tracts (Brunk, 1973)]. If these sequences are more rapidly degraded by exonuclease III, the smaller DNA fragments on our gels would be enriched in repair-incorporated label following low extents of digestion. Indeed Linxweiler & Horz (1982) have reported that, under certain conditions, exonuclease III cleaves cytosine residues most rapidly and guanine residues the slowest. These authors also reported that adenine-rich strands are digested about twice as rapidly as thymidine-rich strands. These results may explain the small, yet reproducible, increase in the $^3H/^{14}C$ ratio we observed following increasing times of digestion (see Results). However, this small change in the data is in the opposite direction predicted for the selective degradation of repair patches to small fragment sizes (above). Furthermore, the $^3H/^{14}C$ ratio of the 146-base band remained constant with increasing extents of exonuclease III digestion (unpublished results; however, see Figures 8 and 10). This ratio should have decreased relative to the undigested core DNA, with increasing digestion by exonuclease III if indeed the repair patches were selectively degraded. Finally, we have observed a decrease in the $^3H/^{14}C$ ratio (i.e., a randomization) in core DNA isolated from cells exposed to long chase times following the pulse-labeling period (see below). It is difficult to imagine how the selective digestion of newly repaired DNA sequences could explain this time-dependent change in the $^3H/^{14}C$ ratio curves. Thus, the possibility that our results can be explained by a sequence bias in the DNA fragment population produced by exonuclease III is unlikely.

The most likely explanation of our exonuclease III digestion results is that the distribution of repair-incorporated label is nonuniform in nucleosome core DNA. This is the case for cells harvested either immediately after a 30-min pulse-labeling period (Figure 8) or following a short chase period prior to harvest (Figure 10). Furthermore, similar results were obtained for cells labeled in the presence or absence of 2 mM hydroxyurea (Figures 8 and 10). The shape of these curves indicates that the core DNA contains repair-incorporated label at both the 5′ and 3′ ends and is approximated best by model II in Figure 5. Analysis of the data, for this general distribution model, yielded values of 62 bases and 114 bases for R1 and R2, respectively. Thus, for this model, the data are best fit by a distribution where repair-incorporated label extends 62 bases into the core DNA from the 5′ end and from 114 bases to the 3′ end with a gap in the distribution between positons 62 and 114. It is interesting to note that these values are not very different from those obtained from our analysis of the DNase I digestion profiles for the distribution in model II (i.e., R1 $\simeq$ 50 and R2 $\simeq$ 90 bases). This result indicates that the small differences in the DNase I digestion profiles of core particles *and* nuclei can essentially be accounted for by this nonuniform distribution.

Given the above distribution and the assumption that linker DNA regions contain the same leves of repair-incorporated nucleotides as the ends of the core DNA, we can calculate the expected relative nuclease sensitivity of repaired DNA (i.e., the ratio of the fraction of repaired DNA that is nuclease-sensitive to the fraction of bulk DNA that is nuclease-sensitive; see the introduction) once these regions are folded into nucleosomes. Clearly, if the nuclease sensitivity of the linker and core DNA in these newly repaired regions is the same as in bulk chromatin, the relative nuclease sensitivity will be greater than 1.0 since the linker DNA is "weighted" more by repair-incorporated label. The fraction of bulk DNA that is nuclease-sensitive can be approximated by the average linker length (47 bp) divided by the average nucleosome repeat length (193 bp) for these cells (Smerdon et al., 1978), or 0.24. The fraction of repaired DNA that is nuclease-sensitive will be

47/(193 − 52) or 0.33. Thus, the predicted relative nuclease sensitivity is 0.33/0.24 or 1.4. This value is within the range measured for the relative nuclease sensitivity immediately following the rapid phase of rearrangement (see the introduction) and, therefore, can also account for this observation.

One can also calculate the fraction of repair synthesis in the core region of nucleosomes that is expected for the above distribution, following the rapid phase of rearrangement. The total amount of nucleosome DNA containing repair label (again, assuming linker DNA contains the same level of repair synthesis as the core DNA ends) is 193 bp − 52 bp = 141 bp. Therefore, the fraction of total repair-incorporated label associated with nucleosome core particles will be (146 − 52)/141 = 0.67. This value should be close to the value obtained for cells chased for a short time after the pulse-labeling period (i.e., where the rapid phase of rearrangement is complete and very little of the slow phase has taken place). Therefore, we determined this fractional value for the core DNA from cells chased for 2.5 h after the 30-min pulse-labeling period (Figure 10). This calculation (using eq B6 of the supplementary material) yields a value of 0.65. [Note that 0.65(193/146) = 0.86 is the value of the ratio discussed in the introduction.] Once again, the distribution obtained from our exonuclease III analysis yields a predicted value (0.67) that is very close to the measured value (0.65). Furthermore, this result rules out the possibility that repair synthesis (at early time after damage) is uniform and our results are due to a very slow re-formation of those nucleosomes repaired in the 52-base central region. In this case, following a 2.5-h chase period, the fraciton of total repair synthesis in core DNA should be close to (146 − 52)/193 = 0.49, a value that is significantly different from the value measured. Thus, most, if not all, of the quantitative differences observed between bulk chromatin and regions of chromatin repaired immediately after DNA damage (and following the rapid phase of rearrangement) can be accounted for by the nonuniform distribution of repair synthesis in nucleosome core DNA reported in this paper.

One obvious explanation for this nonuniform distribution of repair-incorporated nucleotides is a nonuniform distribution of UV-induced lesions in the DNA of nucleosomes. However, consideration of data in the literature does not support this possibility (Williams & Friedberg, 1979; Snapka & Linn, 1981; Niggli & Cerutti, 1982). Snapka & Linn (1981) reported that the level of pyrimidine dimers in the nucleosome core DNA of SV40 minichromosomes, irradiated in vitro with 254-nm light, is ~1.8-fold *greater* than that of free DNA following low UV doses (i.e., <40 J/m^2). At higher UV doses, these authors found comparable levels of pyrimdine dimers in the core particle and free DNA samples. In a study using conditions more like those of our present study, Niggli & Cerutti (1982) examined the concentration of *cis-syn*-cyclobutylthymine dimers in nucleosome core particles and total DNA from UV-irradiated human fibroblasts. These authors found identical levels of thymine dimers in core particle and total DNA for three different doses of 254-nm light. If thymine dimers were uniformly distributed in the 141 bases of nucleosomal DNA (i.e., core plus linker) that contain repair-incorporated label and absent from the 52 bases of DNA devoid of repair label, the concentration of thymine dimers in core DNA should be 12% less than that of total DNA [i.e., 94/146 vs. (94 + 47)/193]. Given the small amout of error in the HPLC analysis of Niggli & Cerutti (1982; see discussion on p 1220 of that paper), these authors should have detected such a difference between the core DNA and total DNA populations. Of course, the above distribution for pyrimidine

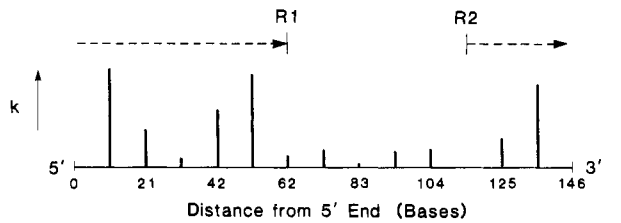

FIGURE 11: Correlation between the predicted distribution of UV-induced repair synthesis in nucleosome core DNA (dashed lines) and the DNase I cutting frequencies (k) obtained by Lutter (1978) for isolated core particles in vitro. The arrows on the dashed lines denote that repair synthesis is in a 5′ → 3′ direction. Redrawn (with permission), with modifications, from Figure 5 of Lutter (1978).

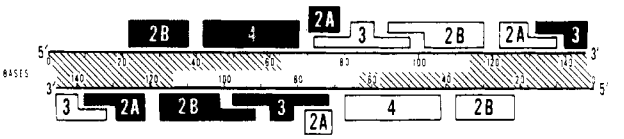

FIGURE 12: Correlation between the predicted distribution of UV-induced repair synthesis in nucleosome core DNA (hatched bars) and the generalized model of Mirzabekov (1980, 1981) for the symmetrical arrangement of core histone binding sites along both strands of core DNA. Redrawn (with permission), with modifications, from Figure 1 of Mirzabekov (1981).

dimers represents an extreme, and the possibility that lower levels of pyrimidine dimers (as well as other UV photoproducts) are produced in the 52-base central region of the core DNA cannot be excluded since the methods used to measure these lesions may not have been sensitive enough to detect such small differences. In any event, this explanation would require that one of the DNA strands have enhanced photolability in the same region that the complementary strand does not (i.e., the ~30 bases of DNA between positions 34 and 62 from the 5′ end; see Figure 12).

An alternative explanation of our results comes from the comparison of the distribution of repair synthesis that we obtain to the DNase I cutting frequencies obtained by Lutter (1978) for isoalted core particles and the proposed histone–DNA binding pattern of Mirzabekov (1980, 1981). As shown in Figure 11, the regions predicted to contain high levels of repair synthesis also contain all of the high-frequency DNase I cutting sites, and conversely, the 52-base central region devoid of repair synthesis contains six of the seven lowest frequency cutting sites. This correlation may reflect a similarity between the constraints placed upon the endonucleolytic action of DNase I in vitro and the process of excision repair in intact cells. Indeed, since excision repair is initiated by an endonucleolytic cut in the damaged DNA strand, the distribution of repair synthesis may be dictated by constraints placed upon the repair endonuclease. In this case, the "mode of constraint" would be the same as that of DNase I in vitro. Figure 12 shows the alignment of the predicted regions of high and low levels of repair synthesis with the histone–DNA binding pattern proposed by Mirzabekov (1980, 1981). As can be seen, the 52-base central region devoid of repair synthesis includes the only "internal" locations where two (rather than one) histones interact with a 10-base segment of each DNA strand (i.e., segments 70–80 and 90–100). Furthermore, the ~25-base "overlap" region, which has reduced repair synthesis on both strands of the helix, contains the only segment in this pattern with two histones binding each of the DNA strands. Thus, the presence of strong histone–DNA interactions in the 62–114-base central region may inhibit the unfolding of DNA from this region of the core particle and present a block to repair polymerases and/or exonucleases. In fact, such a block

Table I: Reported Amounts of UV Damage Removed during the Rapid Phase of Excision Repair in Human Cells

cells[a]	dose (J/m^2)	method[b]	% rapidly removed[c]	ref
HDF	12.5	ESS	62	Paterson et al. (1973)
HDF	10–20	TLC	74	Amacher et al. (1977)
HDF	10	ESS	70–75	Kantor & Setlow (1981)
HeLa	10	RIA	73	Mitchell et al. (1982)
HDF	10	RIA	70	Clarkson et al. (1983)

[a] HDF represents human diploid fibroblasts. [b] Abbreviations for methods used to monitor UV damage: ESS, endonuclease sensitive sites; TLC, thin-layer chromatography; RIA, radioimmunoassay. [c] The percent of UV damage rapidly removed was determined from the extrapolation of the data in the slow-phase portion of the rate curves to zero time.

may be an important factor in "containing" the repair synthesis event to a small region of the genome. Regardless of the mechanism, this "structural constraint" hypothesis requires that DNA damage be removed from the ends of the core DNA more rapidly than from the central 52-base region. Furthermore, the distribution of repair synthesis occurring at long times after damage should be different from that obtained in this paper for repair occuring immediately after damage. Studies examining these possibilities are currently under way.

It is intriguing to speculate that the well-documented rapid and slow phases of excision repair of UV damage in mammalian cells (Cornelis, 1978; Williams & Cleaver, 1978; Konze-Thomas et al., 1979; Zelle & Lohman, 1979; Klocker et al., 1982; references in Table I) reflect the differential repair between the central core region and the remainder of the nucleosome DNA. If the two phases were entirely due to this effect, ~73% of the UV damage should be removed rapidly in human cells and the remaining ~27% of the UV damage should be removed slowly. From the studies referenced above, those reporting on the damage of either human diploid fibroblasts or HeLa cells (which should remove ~72% of the UV damage during the fast repair phase for a nucleosome repeat length of 186 bp; McGhee et al., 1983) and using a UV dose of 10–15 J/m^2 (i.e., similar to this paper) are listed in Table I. As can be seen, the values obtained by four different laboratories using three different techniques to measure UV-induced lesions fall in the range of 62–75% with a mean of 70%. This value is remarkably similar to the 73% predicted by the nonuniform distribution reported here. Clearly, examination of the nucleosomal distribution of repair synthesis occuring at late times after UV damage should indicate whether the two different rates of UV-induced repair are indeed controlled by structural constraints at the nucleosome level.

Finally, it is important to note that in this paper we have examined the distribution of repair sythesis in nucleosomes only for short times after the refolding event (i.e., following short chase periods). These studies do not address the question of stability of nucleosome placement at the repair patches during long times after repair. That is, do nucleosomes move along the DNA during longer time periods causing a randomization of the nonuniform distribution of repaired DNA. Such a nucleosome movement could be caused by long-range perturbations in the nucleofilament resulting from repair taking place at distant sites, or a constitutive process involving nucleosome motion as a normal process within chromatin. Furthermore, such a randomization could explain the slow phase of nucleosome rearrangement discussed in the introduction. We are presently examining this possibility by measuring the distribution of repair synthesis in nucleosome cores from cells chased for long periods of time after the pulse-labeling period. Our results indicate that after long chase periods the distribution of repair-incorporated nucleotides in core DNA is indeed more random than the distribution obtained following short chase periods (K. Nissen, S. Lan, and M. Smerdon, unpublished results). From the present study, however, our data suggest that the refolding of newly rapaired DNA into a nucleosome structure must involve the placement of core histones in a position that is at least close to their original position along the DNA helix (i.e., prior to UV damage). Clearly, if the core particles re-formed at any position along the newly repaired DNA, then the distribution would be randomized. Thus, the fact that we obtain a nonrandom distribution following the refolding event suggests that at least some of the initial distribution is "preserved" during the refolding process. [One might imagine that the adjacent nucleosomes (i.e., those on each side of a repair patch) constrain the replacement of histone–DNA contacts to their original positions following the excision repair event.] This conclusion differs from that of Zolan et al. (1982), who found that repair patches incorporated into regions damaged by angelicin become associated with staphylococcal nuclease resistant DNA at the same rate as repair patches incorporated at UV-damaged sites. Since angelicin adducts were preferentially located in linker DNA and UV-induced pyrimidine dimers are randomly distributed (see earlier discussion), these authors concluded that nucleosome cores do not re-form at their original positions after DNA is repaired. However, the demonstration that angelicin adducts were associated with DNA preferentially digested by staphylococcal nuclease does not establish that these adducts are located exclusively in linker DNA, nor does it establish that repair patches inserted during repair of angelicin adducts are confined to linker DNA. Repair synthesis may *initiate* within linker DNA, or at the ends of core particles, and extend into the core region. This possibility seems more likely when one considers the fact that linker DNA in human cells varies from a maximum of about 50 bp to essentially 0 bp in length and the average repair patch size appears to be ≥35 bases in length (Francis et al., 1981; Th'ng & Walker, 1983). Furthermore, our results indicate that repair patches inserted immediately after UV damage are, in effect, preferentially located in linker DNA and are more nuclease-sensitive than bulk DNA following their refolding into nucleosomes. Since the nuclease sensitivity of repair patches inserted after angelicin damage was identical with that of UV-induced repair synthesis following nucleosome formation (and, therefore, not randomly distributed; Zolan et al., 1982), the distribution of angelicin-induced repair synthesis may, in fact, be the same as reported here.

ACKNOWLEDGMENTS

We thank Drs. Raymond Reeves and Michael Kahn for many helpful discussions during the course of this work and for their critical reviews of the manuscript. We also thank Donald Apple for his help in using the NMR computer program for the analysis of DNase I gel profiles and Dr. Scot Wherland for his help in using the computer program for the curve-fitting analysis of the exonuclease III digestion data. We dedicate this paper in memory of Dr. Irvin Isenberg, Professor of Biophysics, Oregon State University.

APPENDIX

This section shows the development of the equations used to fit the normalized ratio data assuming the distributions given in Figure 5.

Consider the distribution in model II. If we let X represent the distance (in bases) from the 5′ end of the core DNA and

α = R2 − R1, then the ratio of the amount of ^3H label in a fragment X bases long (^3H_X) and the total amount of ^3H label in the core DNA ($^3H_{core}$) is

$$^3H_X/^3H_{core} = \begin{cases} X/(146-\alpha) & X < R1 \\ R1/(146-\alpha) & R1 \leq X \leq R2 \\ (X-\alpha)/(146-\alpha) & X > R2 \end{cases} \quad (A1)$$

Furthermore, the ratio of the amount of ^{14}C label in a fragment X bases long ($^{14}C_X$) and the total amount of ^{14}C label in the core DNA ($^{14}C_{core}$) is

$$^{14}C_X/^{14}C_{core} = X/146 \quad (A2)$$

for all X. Therefore

$$\frac{^3H_X/^{14}C_X}{^3H_{core}/^{14}C_{core}} = \begin{cases} 146/(146-\alpha) & X < R1 \\ 146R1/[X(146-\alpha)] & R1 \leq X \leq R2 \\ 146(X-\alpha)/[X(146-\alpha)] & X > R2 \end{cases} \quad (A3)$$

This equation yields the dependence of the normalized ratio on R1, R2, and the DNA fragment size (X bases long), for model II. Similarly, for model I

$$\frac{^3H_X/^{14}C_X}{^3H_{core}/^{14}C_{core}} = \begin{cases} 0 & X < R1 \\ 146(X-R1)/(\alpha X) & R1 \leq X \leq R2 \\ 146/X & X > R2 \end{cases} \quad (A4)$$

Supplementary Material Available

Details of the method of analysis of the DNase I gel profiles and the method for correction of the ^3H data for the contribution of DNA replicative synthesis including six figures (19 pages). Ordering information is given on any current masthead page.

References

Amacher, D. E., Elliott, J. A., & Lieberman, M. W. (1977) *Proc. Natl. Acad. Sci. U.S.A. 74*, 1553–1557.

Bevington, P. R. (1969) *Data Reduction and Error Analysis for the Physical Sciences*, McGraw-Hill, New York.

Bodell, W. J., & Cleaver, J. E. (1981) *Nucleic Acids Res. 9*, 203–213.

Brunk, C. F. (1973) *Nature (London), New Biol. 241*, 74–76.

Cartwright, I. L., Abmayer, S. M., Fleischmann, G., Lowenhaupt, K., Elgin, S. C. R., Keene, M. A., & Howard, G. C. (1982) *CRC Crit. Rev. Biochem. 13*, 1–86.

Clarkson, J. M., Mitchell, D. L., & Adair, G. M. (1983) *Mutat. Res. 112*, 287–299.

Cornelis, J. J. (1978) *Biochim. Biophys. Acta 521*, 134–143.

Donelson, J. E., & Wu, R. (1972) *J. Biol. Chem. 247*, 4661–4668.

Francis, A. A., Snyder, R. D., Dunn, W. C., & Regan, J. D. (1981) *Mutat. Res. 83*, 159–169.

Garoff, H., & Ansorge, W. (1981) *Anal. Biochem. 115*, 450–457.

Hanawalt, P. C. (1977) in *DNA Repair Processes* (Nichols, W. W., & Murphy, D. G., Eds.) pp 1–19, Symposia Specialists, Miami.

Hanawalt, P. C., Cooper, P. C., Ganesan, A. K., & Smith, C. A. (1979) *Annu. Rev. Biochem. 48*, 783–836.

Igo-Kemenes, T., Horz, W., & Zachau, H. G. (1982) *Annu. Rev. Biochem. 51*, 89–121.

Jack, P. L., & Brookes, P. (1982) *Carcinogenesis 3*, 341–344.

Kaneko, M., & Cerutti, P. A. (1980) *Cancer Res. 40*, 4313–4319.

Kaneko, M., & Cerutti, P. A. (1982) *Chem.-Biol. Interact. 38*, 261–274.

Kantor, G. J., & Setlow, R. B. (1981) *Cancer Res. 41*, 819–825.

Klocker, H., Auer, B., Burtscher, H. J., Hirsch-Kauffman, M., & Schweiger, M. (1982) *Mol. Gen. Genet. 188*, 309–312.

Konze-Thomas, B., Levinson, J. W., Mahér V., & McCormick, J. J. (1979) *Biophys. J. 28*, 315–326.

Lieberman, M. W. (1976) *Int. Rev. Cytol. 45*, 1–23.

Lieberman, M. W., Smerdon, M. J., Tlsty, T. D., & Oleson, F. B. (1979) in *Environmental Carcinogenesis* (Emmelot, P., & Kriek, E., Eds.) pp 345–363, Elsevier/North-Holland Biomedical Press, Amsterdam.

Linxweiler, W., & Horz, W. (1982) *Nucleic Acids Res. 10*, 4845–4859.

Lutter, L. C. (1978) *J. Mol. Biol. 124*, 391–420.

Lutter, L. C. (1979) *Nucleic Acids Res. 6*, 41–56.

Maniatis, T., Jeffrey, A., & van deSande, H. (1975) *Biochemistry 14*, 3787–3794.

McGhee, J. D., Nickol, J. M., Felsenfeld, G., & Rau, D. C. (1983) *Cell (Cambridge, Mass.) 33*, 831–841.

Mirzabekov, A. D. (1980) *Q. Rev. Biophys. 13*, 255–295.

Mirzabekov, A. D. (1981) *Trends Biochem. Sci. (Pers. Ed.) 6*, 240–242.

Mitchell, D. L., Nairn, R. S., Alvillar, J. A., & Clarkson, J. M. (1982) *Biochim. Biophys. Acta 697*, 270–277.

Niggli, H. J., & Cerutti, P. A. (1982) *Biochem. Biophys. Res. Commun. 105*, 1215–1223.

Oleson, F. B., Mitchell, B. L., Dipple, A., & Lieberman, M. W. (1979) *Nucleic Acids Res. 7*, 1343–1361.

Paterson, M. C., Lohman, P. H. M., & Sluyter, M. L. (1973) *Mutat. Res. 19*, 245–256.

Prunell, A., & Kornberg, R. D. (1977) *Cold Spring Harbor Symp. Quant. Biol. 42*, 103–108.

Prunell, A., & Kornberg, R. D. (1982) *J. Mol. Biol. 154*, 515–523.

Prunell, A., Kornberg, R. D., Lutter, L., Klug, A., Levitt, M., & Crick, F. H. C. (1979) *Science (Washington, D.C.) 204*, 855–858.

Reeves, R. (1984) *Biochim. Biophys. Acta 782*, 343–393.

Riley, D., & Weintraub, H. (1978) *Cell (Cambridge, Mass.) 13*, 281–293.

Setlow, R. B. (1980) in *DNA Repair and Mutagenesis in Eukaryotes* (Generoso, W. M., Shelby, M. D., deSerres, F. J., Eds.) pp 45–54, Plenum Press, New York.

Sidik, K., & Smerdon, M. J. (1984) *Carcinogenesis 5*, 245–253.

Simpson, R. (1978) *Cell (Cambridge, Mass.) 13*, 691–699.

Smerdon, M. J. (1983) *Biochemistry 22*, 3516–3525.

Smerdon, M. J. (1985) *J. Biol. Chem.* (in press).

Smerdon, M. J., & Lieberman, M. W. (1978) *Proc. Natl. Acad. Sci. U.S.A. 75*, 4238–4241.

Smerdon, M. J., & Lieberman, M. W. (1980) *Biochemistry 19*, 2992–3000.

Smerdon, M. J., & Lieberman, M. W. (1981) *J. Biol. Chem. 256*, 2480–2483.

Smerdon, M. J., Tlsty, T. D., & Lieberman, M. W. (1978) *Biochemistry 17*, 2377–2386.

Smerdon, M. J., Kastan, M. B., & Lieberman, M. W. (1979) *Biochemistry 18*, 3732–3739.

Smerdon, M. J., Watkins, J. F., & Lieberman, M. W. (1982a) *Biochemistry 21*, 3879–3885.

Smerdon, M. J., Lan, S. Y., Calza, R. E., & Reeves, R. (1982b) *J. Biol. Chem. 257*, 13441–13447.

Smith, S. S., Gilroy, T. E., & Ferrari, F. A. (1983) *Anal. Biochem. 128*, 138–151.

Snapka, R. M. & Linn, S. (1981) *Biochemistry 20*, 68–72.

Th'ng, J. P. H., & Walker, I. G. (1983) *Carcinogenesis 4*, 975–978.
Thomas, K. R., & Olivera, B. M. (1978) *J. Biol. Chem. 253*, 424–429.
Tlsty, T. D., & Lieberman, M. W. (1978) *Nucleic Acids Res. 5*, 3261–3273.
Williams, J. I. & Cleaver, J. E. (1978) *Biophys. J. 22*, 265–279.
Williams, J. I., & Friedberg, E. C. (1979) *Biochemistry 18*, 3965–3972.
Wu, R., Ruben, G., Siegel, B., Jay, E., Spielman, P., & Tu, C. D. (1976) *Biochemistry 15*, 734–740.
Zelle, B., & Lohman, P. H. M. (1979) *Mutat. Res. 62*, 363–368.
Zolan, M. E., Smith, C. A., Calvin, N. M., & Hanawalt, P. C. (1982) *Nature (London) 299*, 462–464.

Contribution of Water to Free Energy of Hydrolysis of Pyrophosphate†

Leopoldo de Meis,* Maria Isabel Behrens, and Jorge H. Petretski
Instituto de Ciências Biomédicas, Departmento de Bioquímica, Universidade Federal do Rio de Janeiro, Cidade Universitária, Rio de Janeiro, RJ, Brazil
Mario J. Politi
Departamento de Bioquimica, Universidade de São Paulo, São Paulo, SP, Brazil
Received May 8, 1985

ABSTRACT: The energy of hydrolysis of phosphate compounds varies depending on whether they are in solution or bound to the catalytic site of enyzmes. With the purpose of simulating the conditions at the catalytic site, the observed equilibrium constant for pyrophosphate hydrolysis (K_{obsd}) was measured in aqueous mixtures of dimethyl sulfoxide, ethylene glycol, or polymers of ethylene glycol. The reaction was catalyzed by yeast inorganic pyrophosphatase at 30 °C. All the cosolvents used promoted a decrease of K_{obsd}. Polymers of ethylene glycol were more effective than dimethyl sulfoxide or ethylene glycol in decreasing K_{obsd}. The higher the molecular weight of the polymer, the lower the value of K_{obsd}. A decrease in K_{obsd} from 346 M ($\Delta G°_{obsd}$ = −3.5 kcal mol^{-1}) to 0.1 M ($\Delta G°_{obsd}$ = 1.3 kcal mol^{-1}) was observed after the addition of 50% (w/v) poly(ethylene glycol) 8000 to a solution containing 0.9 mM $MgCl_2$ and 1 mM P_i at pH 8.0. The association constants of P_i and pyrophosphate for H^+ and Mg^{2+} were measured in presence of different ethylene glycol concentrations in order to calculate the K_{eq} for hydrolysis of different ionic species of pyrophosphate. A decrease in all the K_{eq} was observed. The results are interpreted according to the concept that the energy of hydrolysis of phosphate compounds depends on the different solvation energies of reactants and products.

In aqueous solutions the hydrolysis of pyrophosphate, ATP, or an acyl phosphate residue is accompanied by a large change in free energy (George et al., 1970; Haynes et al., 1978). In contrast, during the catalytic cycle of enzymes involved in energy transduction, there are steps in which the hydrolysis of these compounds is accompanied by only a small energy change. This includes the yeast inorganic pyrophosphatase (Janson et al., 1979; Springs et al., 1981; Cooperman, 1982), myosin (Bagshaw & Trentham, 1974; Trentham et al., 1976), F_1-ATPase of mitochondria and chloroplasts (Boyer et al., 1973, 1977, 1982), the Ca^{2+}-ATPase of sarcoplasmic reticulum (Masuda & de Meis, 1973; Kanazawa, 1976; de Meis & Vianna, 1979), the (Na + K)ATPase of plasma membrane (Post et al., 1975; Taniguchi & Post, 1975), 3-phosphoglycerate kinase (Nageswara et al., 1978), and pyruvate kinase (Nageswara et al., 1979). At present, it is not known why the K_{eq}[1] for hydrolysis of these compounds varies depending on whether they are in solution or on the enzyme surface. This phenomenon appears to be crucial to the mechanism of energy transduction in the living cell.

A large decrease in the P_i concentration required for the spontaneous formation of an acyl phosphate residue at the catalytic site of the Ca^{2+}-ATPase has been observed when organic solvents such as dimethyl sulfoxide and glycerol are included in the assay medium (de Meis, 1981; de Meis et al., 1980, 1982; Dupont & Pougeois, 1983; Chiesi et al., 1984). This has also been shown for the spontaneous synthesis of "tightly" bound ATP at the catalytic site of F_1-ATPase (Sakamoto & Tonomura, 1983; Yoshida, 1983; Cross et al., 1984; Sakamoto, 1984). These findings raise the possibility that solvent structure might be involved in the decrease of the K_{eq} for hydrolysis of phosphate compounds (de Meis, 1981, 1982, 1984). Water possesses the most cooperative structure of all common solvents, but it is destroyed by organic cosolvents. The chemical reactivity of water molecules is scarcely affected by cosolvents. However, reactions that depend on solvent structure change markedly with cosolvent addition (Arnett & McKelvey, 1966; Arnett, 1967; Tan & Lovrien, 1972; Amis & Hinton, 1973).

The aim of this study was to ascertain whether or not a change of solvent structure might lead to a large change in the energy of hydrolysis of a phosphate compound. For this purpose, inorganic pyrophosphate was chosen. In the conditions prevailing in the cytosol, the $\Delta G°_{obsd}$ of pyrophosphate hydrolysis is about −4.0 kcal mol^{-1} (de Meis, 1984; Flodgaard

†Supported in part by grants from the Financiadora de Estudos e Projetos (43.83.00520), Brazil, from the Conselho Nacional de Desenvolvimento Científico e Tecnológico, Brazil, from the U.S. Public Health Service (HL 27867), and from the Organization of American States. J.H.P. is supported by a fellowship from CAPES.
* Address correspondence to this author.

[1] Abbreviations: K_{obsd}, observed equilibrium constant; K_{eq}, equilibrium constant; $\Delta G°_{obsd}$, observed standard free energy; PEG, poly(ethylene glycol); MOPS, 3-(*N*-morpholino)propanesulfonic acid; MES, 2-(*N*-morpholino)ethanesulfonic acid; Tris-HCl, tris(hydroxymethyl)aminomethane hydrochloride.

0006-2960/85/0424-7783$01.50/0 © 1985 American Chemical Society